# Characteristic Impedances of Coaxial Structures of Various Cross Section by Conformal Mapping

E. Costamagna and A. Fanni

*Abstract* —**In a recent paper, Pan [1] presented numerical results for the characteristic impedance of a large number of coaxial systems with different geometry, and compared them with earlier published results. Here, the recently developed numerical techniques for the inversion of the Schwarz–Christoffel conformal transformation [2] have been used to compare the results presented in [1]. The results agree very well, thus lending further weight to the two calculation techniques discussed in [1] and [2].**

## I. Introduction

Pan [1] recently obtained simple analytical expressions for accurately and efficiently determining the characteristic impedance of coaxial systems composed of circular and noncircular conductors having a variety of shapes and presented numerical results.

Accurate results can be obtained, in principle, by the numerical inversion techniques, by means of optimization, of the Schwarz–Christoffel conformal transformation described in [2]. Therefore, it seems to be useful to utilize Pan's data to check the reliability of the inversion process for a wide variety of cases, confirming at the same time the accuracy of the data.

The various families of coaxial lines are examined by referring directly to the tables and figures presented in [1]. The dielectric medium is taken to be free space and the values taken for the permittivity and the velocity of light are those used in [3, p. 3]: this observation is important when comparing results that often agree to more than four figures.

## II. Numerical Results

The analyzed structures are represented in Figs. 1 to 4, and the numerical results are shown with previous data [4]–[14] in Tables I to XII.

The arcs of circles are represented by the sides of regular polygons with suitable numbers of sides (up to 128), inscribed in circles with an effective radius chosen such that along each side the mean distance from the center is equal to $r$ (see figures). The arcs of ellipses are represented by nonregular polygons inscribed therein using two different procedures. In the first, their ends subtend identical angles at the structure center, which, in principle, seems to be suitable for both large $r/b$ (see Fig. 3) and large $a/b$ ratios. In the second, the segments define equal angles between one segment and the next, which seems suitable for representing the portion of the ellipse with the greatest curvature and thus for intermediate $r/b$ and small $a/b$ ratios. Of course, for $a/b=1$ the two procedures lead to the same geometry and the conformal transformation results are very close to those for the coaxial line, with maximum errors of the order of some 0.002%.

The polygons used for the effective conformal transformations are the shaded areas in the figures and use clear symmetry conditions. Continuous lines denote electric walls, and dashed lines magnetic walls. Figs. 1 and 2 and Tables I to IX refer to polygonal outer conductors. In the cases of Fig. 1(a), care was taken to keep the upper electric wall far enough away so as not to affect the first five figures of the results.

Almost all the conformal transformation data in Tables VII, VIII, and IX were obtained in two ways, with nearly coincident results. The first consisted in transforming the polygon of Fig. 2(b), checking that no changes in results were produced by placing an electric or magnetic wall on the vertical side parallel to the trough's bottom wall on the left. The second involved imposing a vertical magnetic wall between the points of shortest distance between the inner and outer conductors and then calculating the impedance of the parallel of the two resulting structures. These structures can, in turn, be referred to Fig. 1(b) and to rectangular outer conductor shapes. (Note that it seems likely that Pan's data [1] for $h/r=0.5$ have been wrongly arranged owing to a clerical error and that they can be rearranged as in Table VII.)

Worthy of mention is the check carried out on the data of Tables IV, V, and VI. For large ratios $r/R$, the increase in capacitance with $r$ is clearly close to twice that calculable for the same variation of $r$ on the geometry of Fig. 1(a) using the single-wire-above-ground formula (2.4.2a) in [3]. Based on this incremental capacitance, an attempt was made to calculate the impedance for $r/R=0.95$ starting from the value obtained by conformal transformation for $r/R=0.9$ and then the impedance for $r/R=0.99$ starting from the value both for $r/R=0.9$ and for $r/R=0.95$. In each case the differences from the tabulated value were less than 0.1% for $a/R=2.5$ and $a/R=2$ and less than 0.5% for $a/R=1.5$. Similar comparisons done starting from the reference data shown in the table were not so satisfactory when the values deviated appreciably from those calculated by conformal transformation. The same type of check has been successfully performed also on the data of Tables VII, VIII, and IX.

As far as we are aware, the data given in Table X for the elliptical structures in Fig. 3 are among the first that can confirm the data published by Pan [1]. They have been obtained with the first of the above-mentioned procedure, which seems to be more insensitive to the number of segments employed.

Fig. 4 and Tables XI and XII refer to polygonal inner conductors.

Excellent agreement has been found between conformal transformation results and certain data reported by Geyi *et al.* [15, tables 2, 3, and 5] for square outer conductor and elliptical structures (differences not exceeding 0.30%).

These results show accuracies often similar to those obtained with polygons of simpler shapes and a small number of sides, for instance, the rectangular coaxial lines described in [16], for which impedances with five figures coincident with Riblet's table [16, table I] have been computed.

## III. Conclusions

The results derived by numerical inversion of the SC formula show very good agreement with Pan's values: in fact, the differences are limited to within about 0.1–0.5% in many cases and seldom exceed some 1%. This shows, besides the practical usefulness of Pan's analytical expressions, the efficiency of the numerical techniques presented in [2], which make numerical

Manuscript received November 8, 1989; revised January 28, 1991.
The authors are with the Istituto di Elettrotecnica, Università di Cagliari, 09123 Cagliari, Italy.
IEEE Log Number 9144274.

0018-9480/91/0600-1040$01.00 

TABLE I
CHARACTERISTIC IMPEDANCE FOR AN $N$-REGULAR-POLYGON OUTER CONDUCTOR IN WHICH $N=1$ OR 2

| $N$ | 1 | | | 2 | | |
|---|---|---|---|---|---|---|
| $r/R$ | Present Work | Pan [1] | Gunston [3, p. 11] | Present Work | Pan [1] | Wheeler [4] |
| 0.05 | 221.11 | 221.12 | 221.12 | 194.08 | 194.08 | 194.08 |
| 0.1 | 179.45 | 179.45 | 179.45 | 152.52 | 152.52 | 152.53 |
| 0.3 | 112.34 | 112.34 | 112.34 | 86.62 | 86.59 | 86.62 |
| 0.5 | 78.95 | 78.95 | 78.95 | 55.71 | 55.66 | 55.72 |
| 0.7 | 53.69 | 53.69 | 53.69 | 34.51 | 34.51 | 34.54 |
| 0.9 | 28.00 | 28.01 | 28.01 | 16.03 | 16.03 | 16.07 |
| 0.95 | 19.37 | 19.37 | 19.37 | 10.63 | 10.64 | 10.67 |

TABLE II
CHARACTERISTIC IMPEDANCE FOR AN $N$-REGULAR-POLYGON OUTER CONDUCTOR IN WHICH $N=3$

| $r/R$ | Present Work | Pan [1] | Seshadri [5] | Epele [6] |
|---|---|---|---|---|
| 0.05 | 187.04 | 187.04 | 187.32 | |
| 0.1 | 145.48 | 145.48 | 145.70 | 145.50 |
| 0.3 | 79.62 | 79.61 | 79.74 | 79.63 |
| 0.5 | 48.96 | 48.91 | 49.03 | 48.98 |
| 0.7 | 28.53 | 28.43 | 26.57 | 28.53 |
| 0.9 | 12.05 | 11.99 | 12.06 | 12.10 |
| 0.95 | 7.70 | 7.70 | | |

TABLE III
CHARACTERISTIC IMPEDANCE FOR AN $N$-REGULAR-POLYGON OUTER CONDUCTOR IN WHICH $N=4$ OR 6

| $N$ | 4 | | | | 6 | | |
|---|---|---|---|---|---|---|---|
| $r/R$ | Present Work | Pan [1] | Seshadri [5] | Riblet [7] | Present Work | Pan [1] | Seshagiri [8], [1], [3] |
| 0.05 | 184.14 | 184.14 | 184.42 | | 181.84 | 181.82 | 181.64 |
| 0.1 | 142.59 | 142.59 | 142.80 | | 140.25 | 140.26 | 140.01 |
| 0.3 | 76.72 | 76.72 | 76.84 | | 74.39 | 74.40 | 74.04 |
| 0.5 | 46.09 | 46.07 | 46.16 | 46.09 | 43.77 | 43.77 | 43.43 |
| 0.7 | 25.85 | 25.77 | 25.89 | 25.85 | 23.59 | 23.56 | 23.34 |
| 0.9 | 10.13 | 10.06 | 10.15 | 10.13 | 8.35 | 8.30 | 8.25 |
| 0.95 | 6.25 | 6.24 | | 6.25 | 4.86 | 4.85 | 4.83 |

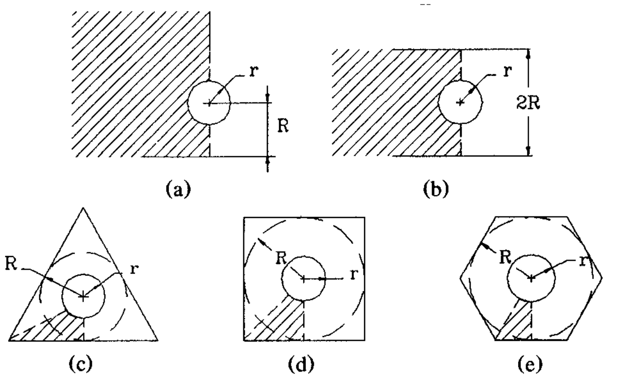


Fig. 1. Outer conductor of regular-polygon cross section for (a) $N=1$, (b) $N=2$, (c) $N=3$, (d) $N=4$, and (e) $N=6$.

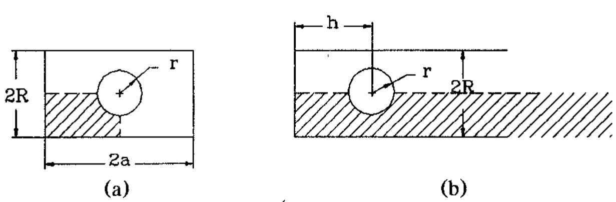


Fig. 2. Outer conductor of nonregular-polygon cross section.

TABLE IV
CHARACTERISTIC IMPEDANCE FOR RECTANGULAR OUTER CONDUCTOR IN WHICH $a/R=1.5$

| $r/R$ | Present Work | Pan [1] | Lin [9] [3, p. 66] | Pan [10], [1] |
|---|---|---|---|---|
| 0.05 | 191.96 | 191.95 | 191.95 | 191.95 |
| 0.1 | 150.39 | 150.39 | 150.39 | 150.46 |
| 0.3 | 84.50 | 84.48 | 84.50 | 84.65 |
| 0.5 | 53.70 | 53.64 | 53.70 | 53.81 |
| 0.7 | 32.86 | 32.72 | 32.82 | 32.94 |
| 0.9 | 15.25 | 14.88 | 15.14 | 15.35 |
| 0.95 | 10.21 | 9.81 | 10.10 | 10.27 |
| 0.99 | 4.35 | 4.12 | 4.31 | 4.36 |

TABLE V
CHARACTERISTIC IMPEDANCE FOR RECTANGULAR OUTER CONDUCTOR IN WHICH $a/R=2$

| $r/R$ | Present Work | Pan [1] | Lin [9] [3, p. 66] | Pan [10], [1] |
|---|---|---|---|---|
| 0.05 | 193.63 | 193.64 | 193.64 | 193.64 |
| 0.1 | 152.08 | 152.08 | 152.08 | 152.13 |
| 0.3 | 86.18 | 86.15 | 86.19 | 86.15 |
| 0.5 | 55.29 | 55.24 | 55.39 | 55.07 |
| 0.7 | 34.17 | 34.14 | 34.48 | 33.86 |
| 0.9 | 15.88 | 15.79 | 16.44 | 15.73 |
| 0.95 | 10.55 | 10.47 | 11.11 | 10.46 |
| 0.99 | 4.42 | 4.42 | 4.80 | 4.39 |

TABLE VI
CHARACTERISTIC IMPEDANCE FOR RECTANGULAR OUTER CONDUCTOR IN WHICH $a/R=2.5$

| $r/R$ | Present Work | Pan [1] | Lin [9] [3, p. 66] | Pan [10], [1] |
|---|---|---|---|---|
| 0.05 | 193.99 | 193.99 | 193.99 | 193.99 |
| 0.1 | 152.43 | 152.43 | 152.43 | 152.44 |
| 0.3 | 86.53 | 86.51 | 86.55 | 86.32 |
| 0.5 | 55.63 | 55.58 | 55.75 | 55.09 |
| 0.7 | 34.44 | 34.43 | 34.82 | 33.78 |
| 0.9 | 16.00 | 15.98 | 16.71 | 15.66 |
| 0.95 | 10.61 | 10.61 | 11.32 | 10.40 |
| 0.99 | 4.43 | 4.48 | 4.90 | 4.37 |

TABLE VII
CHARACTERISTIC IMPEDANCE FOR TROUGH OUTER CONDUCTOR IN WHICH $h/R = 0.5$

| $r/R$ | Present Work | Same, with Parallel | Pan [1] | Chisholm [11] [3, p. 76] |
|---|---|---|---|---|
| 0.025 | 210.32 | 212.57 | 210.34 | |
| 0.05 | 168.72 | 170.53 | 168.75 | 168.72 |
| 0.15 | 102.26 | 103.07 | 102.37 | 102.26 |
| 0.25 | 70.26 | 70.58 | 70.23 | 70.27 |
| 0.35 | 47.31 | 47.40 | 46.71 | 47.41 |
| 0.45 | 25.28 | 25.29 | 23.60 | 26.49 |
| 0.47 | 19.57 | 19.57 | 17.78 | 21.86 |
| 0.49 | | 11.47 | 9.97 | 16.77 |

TABLE VIII
CHARACTERISTIC IMPEDANCE FOR TROUGH OUTER CONDUCTOR IN WHICH $h/R = 1$

| $r/R$ | Present Work | Same, with Parallel | Pan [1] | Chisholm [11] [3, p. 76] | Wheeler [4] |
|---|---|---|---|---|---|
| 0.05 | 188.89 | 188.98 | 188.90 | 188.89 | 188.90 |
| 0.1 | 147.33 | 147.39 | 147.34 | 147.33 | 147.34 |
| 0.3 | 81.36 | 81.37 | 81.47 | 81.36 | 81.39 |
| 0.5 | 50.45 | 50.45 | 50.71 | 50.46 | 50.52 |
| 0.7 | 29.56 | 29.56 | 30.09 | 29.67 | 29.69 |
| 0.9 | 12.41 | 12.41 | 13.13 | 13.24 | 12.56 |
| 0.94 | 8.84 | 8.84 | 9.52 | 10.19 | 8.95 |
| 0.98 | | 4.56 | 5.11 | | 4.61 |

TABLE IX
CHARACTERISTIC IMPEDANCE FOR TROUGH OUTER CONDUCTOR IN WHICH $h/R = 1.5$

| $r/R$ | Present Work | Same, with Parallel | Pan [1] | Chisholm [11] [3, p. 76] |
|---|---|---|---|---|
| 0.05 | 193.00 | 193.01 | 193.01 | 193.01 |
| 0.1 | 151.45 | 151.45 | 151.45 | 151.45 |
| 0.3 | 85.55 | 85.55 | 85.54 | 85.55 |
| 0.5 | 54.69 | 54.69 | 54.65 | 54.69 |
| 0.7 | 33.66 | 33.66 | 33.62 | 33.69 |
| 0.9 | 15.63 | 15.63 | 15.46 | 16.07 |
| 0.94 | 11.55 | 11.55 | 11.36 | 12.46 |
| 0.98 | | 6.32 | 6.19 | |

TABLE X
CHARACTERISTIC IMPEDANCE FOR ELLIPTICAL OUTER CONDUCTOR

| $a/b$ | 1.5 | | 2 | | | 3 | | 5 | |
|---|---|---|---|---|---|---|---|---|---|
| $r/R$ | Present Work | Pan [1] | Present Work | Pan [1] | $r/R$ | Present Work | Pan [1] | Present Work | Pan [1] |
| 0.05 | 188.25 | 188.27 | 191.12 | 189.92 | 0.05 | 192.88 | 192.14 | 193.67 | 193.30 |
| 0.1 | 146.69 | 146.71 | 149.56 | 148.36 | 0.1 | 151.33 | 150.58 | 152.11 | 151.74 |
| 0.3 | 80.81 | 80.83 | 83.67 | 82.47 | 0.3 | 85.43 | 84.67 | 86.21 | 85.82 |
| 0.5 | 50.07 | 50.10 | 52.84 | 51.70 | 0.5 | 54.55 | 53.82 | 55.31 | 54.93 |
| 0.7 | 29.44 | 29.53 | 31.94 | 30.98 | 0.7 | 33.47 | 32.88 | 34.15 | 33.86 |
| 0.9 | 12.65 | 12.75 | 14.31 | 13.73 | 0.9 | 15.32 | 14.99 | 15.78 | 15.61 |

TABLE XI
CHARACTERISTIC IMPEDANCE FOR AN $N$-REGULAR-POLYGON INNER CONDUCTOR IN WHICH $N = 3$ OR 4

| $N$ | 3 | | | | 4 | | | | |
|---|---|---|---|---|---|---|---|---|---|
| $ap/R$ | Present Work | Pan [1] | Seshadri [12] | Pan [10] | Present Work | Pan [1] | Seshadri [12] | Lin [13] | Pan [10] |
| 0.05 | 156.87 | 156.87 | 155.20 | 156.87 | 169.66 | 169.66 | 169.57 | 169.67 | 169.66 |
| 0.1 | 115.31 | 115.31 | 113.58 | 115.19 | 128.10 | 128.11 | 127.95 | 128.11 | 128.12 |
| 0.3 | 49.31 | 49.24 | 47.40 | 48.31 | 62.24 | 62.23 | 61.99 | 62.24 | 62.23 |
| 0.4 | 31.29 | 31.01 | 28.86 | 29.65 | 44.98 | 44.94 | 44.70 | 44.97 | 44.92 |
| 0.5 | | | | | 31.51 | 31.40 | 31.20 | 31.49 | 31.38 |
| 0.6 | | | | | 20.19 | 19.87 | 19.76 | 20.03 | 19.95 |
| 0.65 | | | | | 14.77 | 14.24 | 14.08 | | |
| 0.7 | | | | | 7.82 | 6.70 | | 6.28 | 7.32 |

TABLE XII
CHARACTERISTIC IMPEDANCE FOR AN $N$-REGULAR-POLYGON INNER CONDUCTOR IN WHICH $N = 2$ OR 6

| $N$ | 2 | | | | 6 | | | |
|---|---|---|---|---|---|---|---|---|
| $ap/R$ | Present Work | Pan [1] | Gunston [3, p. 80] | Oberhettinger [14], [1] | Present Work | Pan [1] | Seshadri [12] | Pan [10] |
| 0.05 | 221.15 | 221.16 | 221.15 | | 175.95 | 175.95 | | 175.95 |
| 0.1 | 179.60 | 179.60 | 179.60 | | 134.40 | 134.39 | | 134.41 |
| 0.3 | 113.67 | 113.69 | 113.67 | | 68.53 | 68.54 | 68.59 | 68.59 |
| 0.6 | 71.15 | 71.22 | 71.16 | | 26.97 | 26.93 | 26.96 | 27.08 |
| 0.7 | 60.93 | 60.99 | 60.95 | | 17.69 | 17.58 | | 17.79 |
| 0.9 | 40.67 | 40.80 | 40.93 | 40.13 | | | | |
| 0.94 | 35.48 | 36.21 | 36.00 | 35.25 | | | | |
| 0.99 | 24.73 | 25.03 | | 24.71 | | | | |

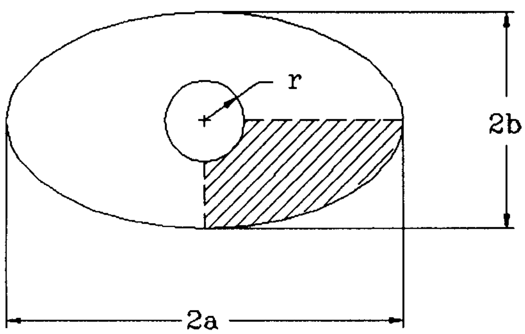


Fig. 3. Outer conductor of elliptical cross section.

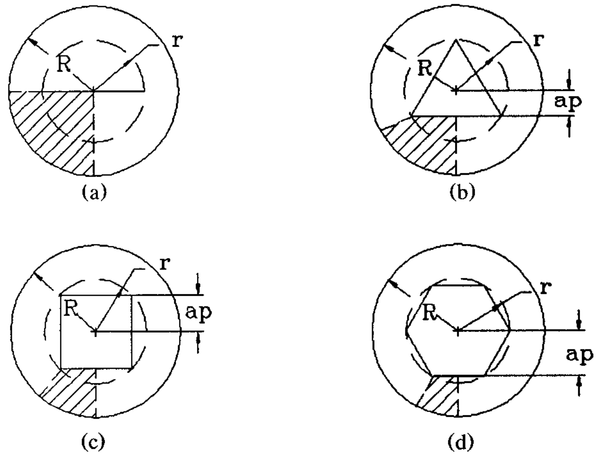


Fig. 4. Inner conductor of regular-polygon cross section for (a) $N=2$, (b) $N=3$, (c) $N=4$, and (d) $N=6$.

inversion by optimization a general-purpose tool very applicable to a broad range of cases.

Indeed, nearly all the structures examined led to large ratios between adjacent sides in the transformed plane of the optimization. These ratios cannot be handled with traditional techniques, but by developing the integration techniques introduced in [2], ratios up to $10^{15}$ have been easily faced. Nevertheless, these conformal mapping techniques often require knowledge of magnetic boundary walls which are not immediately suggested by the geometry of the structure.

## References


[1] S. G. Pan, "Characteristic impedance of a coaxial system consisting of circular and noncircular conductors," *IEEE Trans. Microwave Theory Tech.*, vol. 36, pp. 917–921, May 1988.

[2] E. Costamagna, "On the numerical inversion of the Schwarz-Christoffel conformal transformation," *IEEE Trans. Microwave Theory Tech.*, vol. MTT-35, pp. 35–40, Jan. 1987.

[3] M. A. R. Gunston, *Microwave Transmission-Line Impedance Data.* London: Van Nostrand Reinhold, 1972.

[4] H. A. Wheeler, "Transmission-line properties of a round wire in polygon shield," *IEEE Trans. Microwave Theory Tech.*, vol. MTT-27, pp. 717–721, Aug. 1979.

[5] T. K. Seshadri and K. Rajaiah, "Accurate estimation of characteristic impedance of coaxial transmission-line problems by eigenfunction approach," *Proc. IEEE*, vol. 70, pp. 82–84, Jan. 1982.

[6] L. N. Epele, H. Fanchiotti, and C. A. García Canal, "Characteristic impedance of coaxial lines bounded by $N$-regular polygons," *Proc. IEEE*, vol. 72, pp. 223–224, Feb. 1984.

[7] H. J. Riblet, "An accurate approximation of the impedance of a circular cylinder concentric with an external square tube," *IEEE Trans. Microwave Theory Tech.*, vol. MTT-31, pp. 841–844, Oct. 1983.

[8] N. Seshagiri, "Least-weighted-square method for the analysis and synthesis of transmission lines," *IEEE Trans. Microwave Theory Tech.*, vol. MTT-15, pp. 494–503, Sept. 1967.

[9] W. G. Lin and S. L. Chung, "A new method of calculating the characteristic impedances of transmission lines," *Acta Phys. Sin.*, vol. 19, pp. 249–258, Apr. 1963 (in Chinese). Selected results are quoted in [1, p. 66].

[10] S. G. Pan, "A method of solving coaxial transmission lines of complicated cross-section," *Scientia Sinica*, series A, pp. 205–217, Feb. 1987.

[11] R. M. Chisholm, "The characteristic impedance of trough and slab lines," *IRE Trans. Microwave Theory Tech.*, vol. MTT-4, pp. 166–172, July 1956.

[12] T. K. Seshadri and K. Rajaiah, "Eigenfunction solutions of a class of TEM transmission line," *Proc. Inst. Elec. Eng.*, vol. 131, pt. H, pp. 279–280, Aug. 1984.

[13] W. Lin, "A critical study of the coaxial transmission line utilizing conductors of both circular and square cross-section." *IEEE Trans. Microwave Theory Tech.*, vol. MTT-30, pp. 1981–1988, Nov. 1982.

[14] F. Oberhettinger and W. Magnus, *Applications of Elliptic Functions in Physics and Technology.* New York: Springer, 1949.

[15] W. Geyi, L. Xueguan, and W. Wanchun, "Solution of the characteristic impedance of an arbitrarily shaped TEM transmission line using complex variable boundary element method (CVBEM)," *Proc. Inst. Elec. Eng.*, vol. 136, pt. H, pp. 73–75, Feb. 1989.

[16] H. J. Riblet, "The exact dimensions of a family of rectangular coaxial lines with given impedance," *IEEE Trans. Microwave Theory Tech.*, vol. MTT-20, pp. 538–541, Aug. 1972.


# A Procedure for Solving the Electric Field Integral Equation for a Dielectric Scatterer with a Large Permittivity Using Face-Centered Node Points

Ching-Chuan Su

***Abstract*—A numerical procedure for solving the electric field integral equation (EFIE) using the pulse-basis block model is proposed. The main features of the method are the use of face-centered node points and a unique way of choosing the unknown fields. Such a procedure keeps the resulting matrix relatively well conditioned, even when the magnitude of the permittivity is large. In addition, the proposed procedure can preserve the convolution property contained in the EFIE and, hence, the FFT can be incorporated into the algorithm.**

## I. Introduction

The electric field integral equation (EFIE) is widely employed to analyze inhomogeneous dielectric scatterers of arbitrary shapes. To solve the integral equation numerically the method employing the block model (i.e., using rectangular cells to model an arbitrarily shaped scatterer) in conjunction with the pulse-function expansion and the point-matching technique is rather popular [1]–[7]. Recently, the efficiency of this method with respect to both computational speed and memory requirements has been greatly improved by the use of the conjugate gradient method (CGM) and the fast Fourier transform (FFT) [4]–[6].

Manuscript received March 1, 1990; revised December 31, 1990.
The author is with the Department of Electrical Engineering, National Tsinghua University, Hsinchu, Taiwan.
IEEE Log Number 9144275.